International Journal of Applied Earth Observations and Geoinformation 113 (2022) 102979

Contents lists available at ScienceDirect

International Journal of Applied Earth Observations and Geoinformation

journal homepage: www.elsevier.com/locate/jag

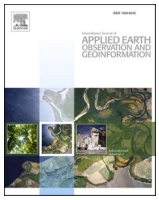

How accurately can we retrieve irrigation timing and water amounts from (satellite) soil moisture?

Luca Zappa [a,*], Stefan Schlaffer [a], Luca Brocca [b], Mariette Vreugdenhil [a], Claas Nendel [c,d,e,f], Wouter Dorigo [a]

[a] Department of Geodesy and Geoinformation, Technische Universitaet Wien, Vienna, Austria
[b] Research Institute for Geo-Hydrological Protection, National Research Council, Perugia, Italy
[c] Leibniz Centre for Agricultural Landscape Research (ZALF), Müncheberg, Germany
[d] Institute of Biochemistry and Biology, University of Potsdam, Potsdam, Germany
[e] Global Change Research Institute, The Czech Academy of Science, Brno, Czech Republic
[f] Integrative Research Institute on Transformations of Human-Environment Systems (IRI THESys), Humboldt Universität zu Berlin, Berlin, Germany

ARTICLE INFO

Keywords:
Remote sensing
Soil moisture
Irrigation
Detection
Quantification
Sentinel-1

ABSTRACT

While ensuring food security worldwide, irrigation is altering the water cycle and generating numerous environmental side effects. As detailed knowledge about the timing and the amounts of water used for irrigation over large areas is still lacking, remotely sensed soil moisture has proved potential to fill this gap. However, the spatial resolution and revisit time of current satellite products represent a major limitation to accurately estimating irrigation. This work aims to systematically quantify their impact on the retrieved irrigation information, hence assessing the value of satellite soil moisture for estimating irrigation timing and water amounts.

In a real-world experiment, we modeled soil moisture using actual irrigation and meteorological data, obtained from farmers and weather stations, respectively. Modeled soil moisture was compared against various remotely sensed products differing in terms of spatio-temporal resolution to test the hypothesis that high-resolution observations can disclose the irrigation signal from individual fields while coarse-scale satellite products cannot. Then, in a synthetic experiment, we systematically investigated the effect of soil moisture spatial and temporal resolution on the accuracy of irrigation estimates. The analysis was further elaborated by considering different irrigation scenarios and by adding realistic amounts of random errors in the soil moisture time series.

We show that coarse-scale remotely sensed soil moisture products achieve higher correlations with rainfed simulations, while high-resolution satellite observations agree significantly better with irrigated simulations, suggesting that high-resolution satellite soil moisture can inform on field-scale (~40 ha) irrigation. A thorough analysis of the synthetic dataset showed that satisfactory results, both in terms of detection (F-score > 0.8) and quantification (Pearson's correlation > 0.8), are found for noise-free soil moisture observations either with a temporal sampling up to 3 days or if at least one-third of the pixel covers the irrigated field(s). However, irrigation water amounts are systematically underestimated for temporal samplings of more than one day, and decrease proportionally to the spatial resolution, i.e., coarsening the pixel size leads to larger irrigation underestimations. Although lower spatial and temporal resolutions decrease the detection and quantification accuracies (e.g., R between 0.6 and 1 depending on the irrigation rate and spatio-temporal resolution), random errors in the soil moisture time series have a stronger negative impact (Pearson R always smaller than 0.85). As expected, better performances are found for higher irrigation rates, i.e. when more water is supplied during an irrigation event. Despite the potentially large underestimations, our results suggest that high-resolution satellite soil moisture has the potential to track and quantify irrigation, especially over regions where large volumes of irrigation water are applied to the fields, and given that low errors affect the soil moisture observations.

* Corresponding author at: Department of Geodesy and Geoinformation, Technische Universitaet Wien, Wiedner Hauptstrasse 8, 1040 Vienna, Austria.
E-mail address: luca.zappa@geo.tuwien.ac.at (L. Zappa).

https://doi.org/10.1016/j.jag.2022.102979
Received 19 January 2022; Received in revised form 22 July 2022; Accepted 12 August 2022
Available online 19 August 2022

1. Introduction

Irrigation represents the single largest human intervention in the water cycle by accounting for around 70 % of freshwater withdrawals worldwide (Campbell et al., 2017; Dorigo et al., 2021). Currently, irrigated agriculture ensures food security worldwide by providing 34 % of the agricultural production (Foley et al., 2011; Siebert and Döll, 2010) and an increase in irrigation demand is projected due to the concurrent effect of global warming, change of precipitation patterns, and rising living standards of a growing population (Eekhout et al., 2018; Kummu et al., 2016; Rockström et al., 2012; Vorosmarty, 2000). However, this extensive use of water is leading to several environmental problems, such as groundwater depletion (Famiglietti, 2014; Wada et al., 2012), soil salinization (Amezketa, 2006), and nitrogen emissions (Deng et al., 2018). Hydrological models simulating the water cycle and the dynamic distribution of terrestrial water fluxes and storages are generally used for informing and driving sustainable management of agricultural water resources. However, despite recent advances in integrating human activities, e.g., irrigation, in such models, the anthropogenic impact on the water cycle remains poorly represented (Modanesi et al., 2022; Puy et al., 2022). Indeed, the vast majority of irrigation water abstractions is not monitored (Brocca et al., 2018; Lopez et al., 2020), hence the spatial and temporal distribution of irrigated fields, and even more notably, the timing of individual irrigation events and the associated amount of water allotted at the field scale, remain largely unknown (Dorigo et al., 2021).

Earth observation satellites provide a unique and convenient means to monitor key processes and state variables related to irrigation. Remote sensing observations from multispectral sensors have been assimilated into water and energy balance models to estimate evapotranspiration (Anderson, 1997; Bastiaanssen et al., 1998; Corbari et al., 2020; Fisher et al., 2017; McCabe et al., 2019, 2016; Miralles et al., 2016). Through additional information, such as rainfall or evapotranspiration modeled without any irrigation input, it is possible to subsequently divide the total evapotranspiration into the rainfed and irrigated portions (Droogers et al., 2010; Peña-Arancibia et al., 2016; Romaguera et al., 2010; van Dijk et al., 2018; van Eekelen et al., 2015). One of the main benefits of optical and infrared sensors is their high spatial resolution (<1 km) and existence of long-term records (>20 years). However, they are affected by cloud cover, which might limit the number of valid observations over certain periods and some regions of the world (Massari et al., 2021). Nonetheless, multispectral remote sensing has been widely adopted to map irrigated areas at national-, continental-, and global-scale (Ambika et al., 2016; Coleman et al., 2020; Deines et al., 2019; Meier et al., 2018; Ozdogan and Gutman, 2008; Thenkabail et al., 2009). In fact, optical and infrared sensors can detect the improved vegetation vigor and health induced by irrigation compared to non-irrigated vegetation, while satellite thermal infrared observations and land surface models can be used to pinpoint regions where anthropogenic activities have a considerable impact on latent heat fluxes (Hain et al., 2015).

In recent years, soil moisture products derived from microwave sensors on board satellites have also been used to estimate irrigation water amounts. Compared to multispectral sensors, microwave observations have the advantage of being mostly insensitive to weather conditions. Various remotely sensed soil moisture products can effectively detect the irrigation timing at the field- and regional- scale (Bazzi et al., 2020; Lawston et al., 2017; Le Page et al., 2020; Zappa et al., 2021). The estimation of irrigation water amounts based on remotely sensed soil moisture has been carried out either by adapting the SM2RAIN algorithm (Brocca et al., 2014) or by quantifying the difference between satellite and modeled soil moisture (Zaussinger et al., 2019). The first approach has been tested initially over nine pilot sites throughout the United States (US), Europe, Africa, and Australia (Brocca et al., 2018) and has been applied to other regions (Dari et al., 2020; Jalilvand et al., 2019; Zhang et al., 2018). The second approach, based on the assumption that modeled soil moisture does not account for artificial water supply while satellite observations incorporate irrigation signals, has been tested over the contiguous US (CONUS) (Zaussinger et al., 2019) and subsequently expanded globally (Zohaib and Choi, 2020). The same hypothesis has been extensively employed also for discriminating irrigated and non-irrigated areas (Escorihuela and Quintana-Seguí, 2016; Kumar et al., 2015; Qiu et al., 2016; Zhang et al., 2018; Zohaib et al., 2019). Using high spatial resolution satellite soil moisture observations, Zappa et al. (2021) proposed a methodology for detecting individual irrigation events and estimating irrigation water amounts based on the different soil moisture dynamics of an irrigated field compared to its surrounding area.

Notwithstanding the promising results obtained by microwave-derived soil moisture for detecting individual events and quantifying irrigation water amounts, satellite products are characterized by a trade-off between spatial and temporal resolution. Hence, detailed knowledge of irrigation features is often constrained by the coarse scale of most soil moisture products (10 to 40 km). Typically, only a limited number of irrigated fields is present within a coarse resolution pixel, which, mixed with non-irrigated fields, water bodies, urban areas, and other artifacts dampens the irrigation signal (Brocca et al., 2018; Zaussinger et al., 2019). Conversely, (quasi-) field-scale soil moisture products, e.g., derived from Sentinel-1 (Bauer-Marschallinger et al., 2019; El Hajj et al., 2017), have longer revisit time and irrigation-driven wetting events might not be captured (Filippucci et al., 2020; Zappa et al., 2021). Downscaling coarse-scale products could be further explored (Alemohammad et al., 2018; Malbéteau et al., 2018; Peng et al., 2017; Sabaghy et al., 2018; Zappa et al., 2019) to obtain soil moisture estimates at appropriate spatio-temporal resolution for irrigation monitoring.

A better knowledge of irrigation practices, i.e., where, when and how much water is employed, can potentially provide valuable insights and actionable data to water managers, as well as offer the hydrological modelling community more realistic representations of human decisions (Massari et al., 2021). In this work, we aim to address the following questions: i) can current satellite soil moisture products observe field-scale irrigation? and ii) how accurate is the estimated irrigation information? To answer such questions, we tested the hypothesis that current high-resolution satellite soil moisture products can disclose the irrigation signal from individual fields using ground reference irrigation data. Furthermore, we quantitatively assessed not only the effect of spatial and temporal resolution, but also the impact of different irrigation rates and the presence of noise in the soil moisture data, on the accuracy of estimated irrigation timing and water amounts.

2. Data & methods

2.1. Test site

Four center-pivot fields located in Germany (51.92° N, 13.07° E) were selected as pilot sites because of the availability of irrigation data (timing and volumes) for the period 2016–2019 (Fig. 1). According to the Koeppen-Geiger classification (Rubel et al., 2017), the site is characterized by a temperate oceanic climate (Cfb class) with mean annual temperature and precipitation of approximately 9 °C and 550 mm, respectively. Soil texture is classified as sandy loam (Ballabio et al., 2016). The mean field size is 40 ha, and the amount of water distributed during each irrigation event was 15 mm. Cultivated crops were mostly potato, winter wheat, and maize.

2.2. Real-world experiment

Satellite products were compared against modeled soil moisture to test the hypothesis that high-resolution satellite observations can disclose the irrigation signal coming from individual fields while coarse-scale products cannot. We selected three satellite soil moisture products characterized by different spatio-temporal resolutions, observation

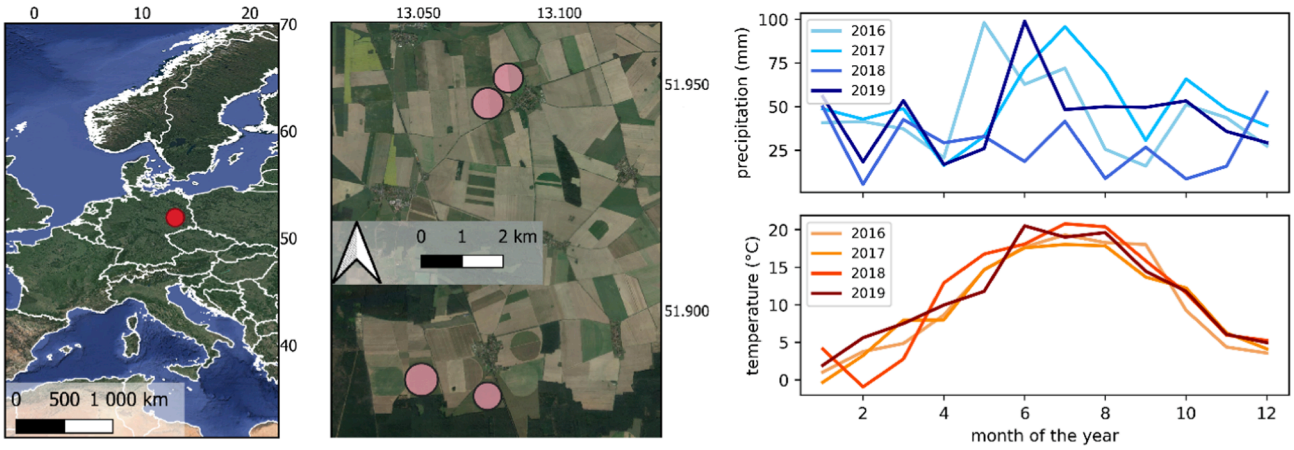

Fig. 1. Location of the test fields in Germany and monthly meteorological parameters (cumulative precipitation and mean air temperature) recorded by a weather station in close proximity.

frequencies, and retrieval algorithms (Table 2). Specifically, we used the Copernicus Global Land Service surface soil moisture product (CGLS-SSM) obtained from Sentinel-1C-band SAR backscatter with the TU Wien change detection method, the ESA CCI combined soil moisture product (CCI version v05.2), which is a merged product of various active and passive microwave soil moisture products, and the SMAP L3 product obtained from an L-band radiometer using the single channel algorithm (SCA). Satellite soil moisture time series were extracted from the pixels whose center was closest to each test field. The irrigated fraction within the selected satellite pixels ranges between 20 % and 60 % for the CGLS-SSM, while it is considerably lower than 1 % for both CCI and SMAP products. The large contrast in irrigated fractions between CGLS-SSM and CCI/SMAP stems from the different spatial resolutions of the products (Table 1).

Soil moisture for the top 10 cm of the soil was simulated over the test fields using the semi-analytical soil water balance model (SWBM) developed by Brocca et al. (2008; 2014). The SWBM model requires as input data only meteorological variables that are routinely measured, i.e., rainfall and air temperature, while model parameters are derived from soil texture information (Brocca et al., 2016). Soil moisture was simulated both with and without irrigation input, hence mimicking the actual status of the irrigated fields as well as rainfed conditions. The model proved to correctly represent soil moisture across different test sites over Europe with correlations higher than 0.8 and root mean square differences lower than 0.025 $m^3\ m^{-3}$ and has been used in numerous studies as reference dataset (Bauer-Marschallinger et al., 2019, 2018; Brocca et al., 2018, 2014, 2011; Jalilvand et al., 2019; Melone et al., 2008; Morbidelli et al., 2011). Meteorological measurements at the test site were obtained from a nearby weather station, while irrigation data, i.e., timing and amount of water supplied, was provided by farmers. The comparison between satellite and model data was carried out on a yearly basis, after considering the model timestamps closest to satellite acquisitions and subsequently scaling satellite observations to match the mean and standard deviation of modeled soil moisture.

2.3. Synthetic experiment

2.3.1. Model simulations

The SWBM was used to further investigate the effect of different variables on the accuracy of the retrieved irrigation information, namely: irrigation water input, spatial and temporal resolution (individually and combined), and noise. We considered scenarios with net irrigation rates of 5, 15, and 25 mm per event to simulate different irrigation systems and farmers' decisions on how much water to supply to the field (Fig. 2). It should be underlined that the entire amount of water is supposed to enter the soil, hence water losses from canopy interception and efficiency of the irrigation system are implicitly accounted for. Therefore, only a portion of the entire amount of irrigation water abducted from water sources can be retrieved, while a more rigorous estimate of total irrigation water, i.e., including losses would require many additional information such as the irrigation system and its maintenance status, the meteorological conditions at the time of irrigation, the type of crop and its phenological status. High irrigation rates can be considered representative of sprinkler and gravity systems, which generally cause a considerable wetting of the topsoil, while low irrigation rates portray drip irrigation systems (Massari et al., 2021).

Soil moisture dynamics mimicking a rainfed scenario were simulated without any irrigation input, while forcing the model with irrigation data provided time series representative of irrigated fields. The latter represents a scenario in which the entire satellite pixel is covered with irrigated land, i.e., the irrigated fraction of the satellite pixel would be 100 %. It should be noted that considering the irrigated fraction allows us to ideally cover all possible combinations of pixel spatial resolution and irrigated area covered by the pixel. For instance, an irrigated area of 50 % might exemplify a 1 km pixel encompassing an irrigated field of 50 ha, as well as a 0.5 m pixel (obtained from, e.g., unmanned aerial vehicles) and the small-scale effects of irrigation, e.g., intra-row variability in a drip irrigation system (Reyes-Cabrera et al., 2016). However, given the constraint in terms of spatial resolution posed by satellite soil moisture products, the focus of this work is given to average field-scale dynamics rather than to within-field variability. Also, because of the minor effect of drip and micro- irrigation systems on field-scale surface

Table 1
Specifications of the satellite soil moisture products that have been compared to modeled soil moisture.

Name	Spatial sampling	Temporal resolution	Reference	Source
CGLS-SSM	1 km	1.5–4 days (over Europe)	Bauer-Marschallinger et al., 2019	https://land.copernicus.eu/global/products/ssm
CCI	0.25°	1 day	Dorigo et al., 2017	https://www.esa-soilmoisture-cci.org/
SMAP	36 km	1–3 days	Entekhabi et al., 2010	https://n5eil01u.ecs.nsidc.org/SMAP/

Table 2
Summary of the simulated soil moisture data tested in the synthetic experiment.

Irrigation input (mm/event)	Temporal sampling (Hours)	Irrigated fraction (%)	Random error (m^3 m^{-3})
5, 15, 25	1, 3, 6, 12, 24, 48, 72, 144	100	0
5, 15, 25	1	100, 90, 70, 50, 30, 10, 5, 1	0
5, 15, 25	24	70	0, 0.04
5, 15, 25	24	30	0, 0.04
5, 15, 25	72	70	0, 0.04
5, 15, 25	72	30	0, 0.04

soil moisture, satellite observations are better suited for monitoring gravity and sprinkler irrigation systems (Zappa et al., 2021; Zaussinger et al., 2019). The simulated soil moisture time series have hourly resolution and are noise-free, representing an ideal scenario. Hence, we investigated the effect of a longer revisit time by downsampling hourly observations to 3, 6, 12, 24, 48, 72, and 144 h. Similarly, we mimicked different satellite pixel sizes by a weighted average of the non-irrigated and the irrigated soil moisture time series so that the latter's contribution, i.e., the irrigated fraction, would increase from 1 % to 100 %. Finally, we explored the combined effect of spatio-temporal resolutions representing current and upcoming high-resolution satellite missions by setting up four custom combinations. In particular, the temporal sampling was either daily (1d) or 3-daily (3d), while the irrigated fraction was either 30 % or 70 %. To obtain more realistic satellite soil moisture observations, we added Gaussian noise with a standard deviation of 0.04 m3/m^{-3}(−|-), which is the target uncertainty of various missions (Gruber et al., 2020), to the irrigated soil moisture time series (Table 2). It is noteworthy that only the random component of the total error characterizing satellite soil moisture observations is taken into account. Systematic errors due to, e.g., the retrieval algorithm, and other autocorrelated errors driven by, e.g., the temporally varying effect of vegetation on the observed signal, are not considered as they are product-specific and difficult to model rigorously (Dong and Crow, 2017; Zwieback et al., 2013).

Overall, 72 combinations encompassing various spatio-temporal resolutions, irrigation scenarios, and random errors were tested. Note that whenever random noise was added to soil moisture time series, the analysis was repeated 100 times to obtain robust results.

2.3.2. *Irrigation detection and quantification*

For the detection of individual irrigation events and the subsequent quantification of net irrigation water amounts, we employed a modified version of the approach presented in Zappa et al. (2021). This method was preferred over alternative approaches because its reliability is not affected by the quality of ancillary data, such as precipitation in the SM2RAIN approach (Brocca et al., 2018) or land surface models (LSM) in the approach of Zaussinger et al. (2019). Furthermore, it is specifically tailored for high-resolution (satellite) soil moisture. The underlying principle of this approach is that the soil moisture temporal behavior of an irrigated field is considerably different compared to its surrounding area, i.e., the regional scale, under the assumption that over a relatively large area most fields are not irrigated simultaneously (Zappa et al., 2021). It should be noted that in the regional soil moisture are included only agricultural fields with similar vegetation conditions as the irrigated field of interest, thus reducing the negative effect of landscape fragmentation. Hence, soil moisture temporal dynamics of an irrigated field should be distinguishable from the regional soil moisture evolution. Based on such a difference, it is possible to determine firstly individual irrigation events and subsequently estimate the amount of irrigation water applied. Here, the regional soil moisture was replaced by model simulations obtained without irrigation (w/o irr), while soil moisture of irrigated fields consisted of model simulations forced with irrigation (w/ irr). A soil moisture increase occurring at timestamp *t* was flagged as an irrigation event if two conditions were satisfied: i) soil moisture of the irrigated field increased between *t-1* and *t* (Eq. (1)), and ii) the ratio between the relative soil moisture increase of the irrigated field and the regional variation (which could be either an increase or a decrease) was larger than a predefined threshold (Eq. (2)). Zappa et al. (2021) investigated the optimal threshold value for irrigation detection

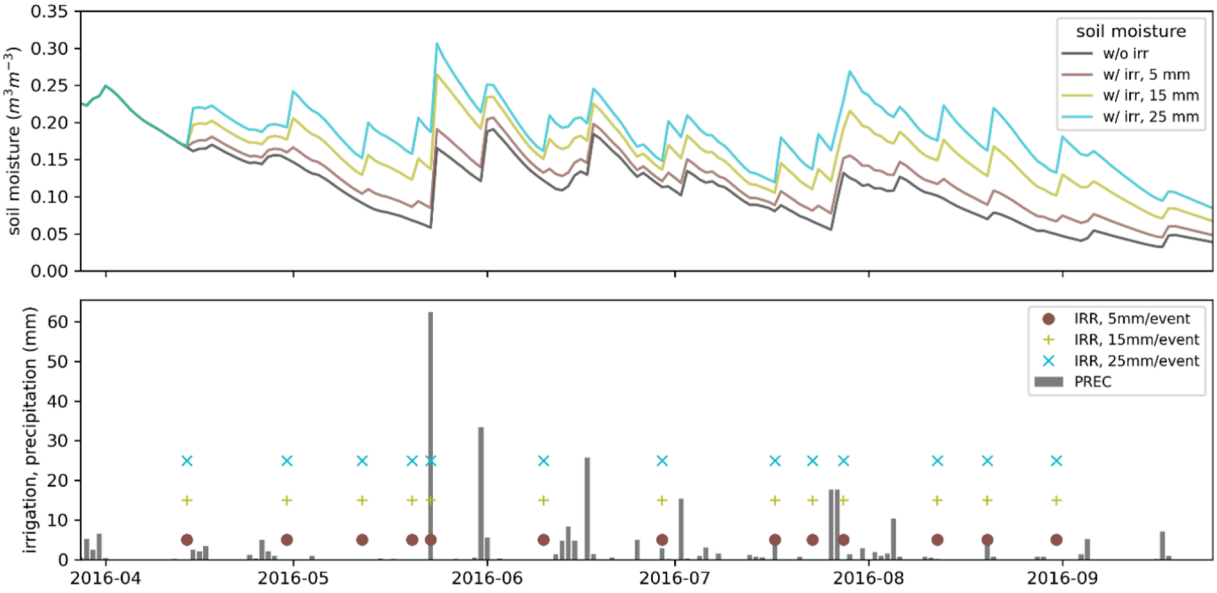

Fig. 2. Soil moisture time series simulated without irrigation (w/o irr) and with different irrigation forcing (w/ irr), i.e., 5, 15, and 25 mm/event, for a center pivot field in Germany. Time series of precipitation and irrigation input are also shown.

and found that a threshold of 1.01 provided the best overall accuracy.

$$SM_t^{w/\,irr} - SM_{t-1}^{w/\,irr} > 0 \quad (1)$$

$$\Delta SM_t^{w/irr}/SM_{t-1}^{w/irr} > 1.01 \cdot \Delta SM_t^{w/oirr}/SM_{t-1}^{w/oirr} \quad (2)$$

where the soil moisture difference at time t (ΔSM_t), is obtained as follow:

$$\Delta SM_t = SM_t - SM_{t-1} \quad (3)$$

We then considered the soil water balance equations of an irrigated field (Eq. (4)) and of its surrounding area (Eq. (5)):

$$\Delta SM_t^{w/irr} = I_t + P_t - ET_t - sr_t - g_t \quad (4)$$

$$\Delta SM_t^{w/oirr} = P_t - ET_t - sr_t - g_t \quad (5)$$

assuming that the irrigation signal of individual fields is negligible in the regional soil moisture dynamics (Eq. (5)). I_t represents the net irrigation, P_t is precipitation, ET_t is the evapotranspiration, sr_t and g_t describe surface runoff and drainage, respectively. Hence, the net amount of water employed for an individual irrigation event, I_t (Eq. (6)), is obtained by subtracting Eq. (5) from Eq. (4):

$$I_t = \Delta SM_t^{w/irr} - \Delta SM_t^{w/oirr} \quad (6)$$

Two important aspects should be noted here. First, Eq. (6) implies that the outflow fluxes (ET_t, sr_t and g_t) are identical between irrigated and non-irrigated fields. This is a simplified representation of real-world conditions where these fluxes are affected, to some degree, by the amount of water in the soil, and hence by irrigation (Brombacher et al., 2022). Second, the present method only accounts for the irrigation water entering the soil, i.e., the net irrigation, while water losses due to leakage, wind drift and canopy interception are not considered (Zappa et al., 2021).

2.3.3. Accuracy assessment

Correctly and wrongly detected events, i.e., true positive (TP) and false positive (FP), were identified. Then, the number of undetected irrigation events, i.e., false negatives (FN), was obtained as the difference between the total number of actual irrigation events and TP. The detection accuracy was assessed considering precision, recall, and F-score. Precision is the ratio between TP and all detected events (TP + FP), while recall is the ratio between TP and all the irrigation events occurring in a field (TP + FN). High precision scores indicate a low probability of false irrigation detection, while high recall values denote a low probability of missing actual irrigation events. For a balanced representation of precision and recall, we also considered the F-score, which is the harmonic mean of precision and recall. The quantification accuracy was evaluated in terms of Pearson's correlation (R), normalized root mean square deviation (nRMSD), and normalized bias (nBIAS) between the reference and estimated yearly irrigation water amounts.

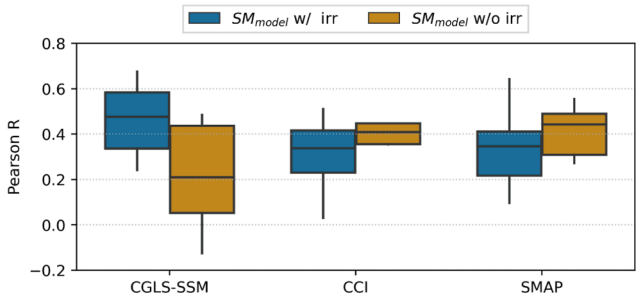

Fig. 3. Pearson's correlation between high-resolution (CGLS-SSM) and coarse-resolution (CCI and SMAP) remotely sensed soil moisture products against soil moisture modeled with (blue boxes) and without (orange boxes) irrigation. Results refer to the four test fields over the investigated period (2016–2019).

nRMSD (nBIAS) was calculated as the ratio between RMSD (bias) and the average yearly irrigation. As both RMSD and bias are proportional to the amplitude of the irrigation forcing, a direct comparison would not be possible. Hence, normalized metrics allow us to compare and simplify the interpretation of results obtained from simulations forced with different irrigation inputs.

3. Results and discussion

3.1. Real-world experiment

Here, we assess the consistency between satellite soil moisture products and model simulations, the latter forced with (w/ irr) and without irrigation (w/o irr) (Fig. 3). Note that actual irrigation data provided by farmers were used as input to the model. It should be emphasized that inherent differences characterize satellite-derived and modeled soil moisture. Model simulations are affected by the model structure, their parameterization, and the quality and representativeness of the forcing data, while remotely sensed products are characterized by errors and uncertainties due to, e.g., the radiometric accuracy of the sensor and the retrieval algorithm used. Furthermore, satellite observations not only contain the irrigation signal from irrigated fields, but also carry information from, e.g., non-irrigated fields, forests, urban areas and water bodies. We found that coarse resolution soil moisture products, i.e., CCI and SMAP, have higher correlations with rainfed simulations. This was expected as the study region is not extensively irrigated (Wriedt et al., 2009), hence large-scale soil moisture dynamics have more resemblance to natural conditions. On the other hand, the CGLS-SSM product shows considerably better agreement with simulations including irrigation than with those without irrigation (median Pearson's R equal to 0.47 and 0.21, respectively). These promising results are obtained in a continental climate, generally characterized by moderate, but heterogeneously distributed precipitation during the growing season (Fig. 1). Hence, better performances are to be expected in arid and semi-arid regions, where the soil moisture difference between irrigated fields and the non-irrigated surrounding area is even larger.

3.2. Synthetic experiment

3.2.1. Impact of temporal and spatial resolution

Fig. 4 shows soil moisture simulated with and without irrigation, together with the actual and estimated irrigation water amounts. Temporally and spatially sub-sampled soil moisture time series are also displayed. Soil moisture observations with 24 h sampling do not show significant differences compared to the hourly dynamics, while with 72 h sampling some irrigation-induced soil moisture increases are only partially captured. These findings suggest that drainage to deeper soil layers and evapotranspiration losses become non-negligible approximately for sampling intervals longer than one day. Soil moisture dynamics for irrigated fractions smaller than 100 % increasingly resemble the rainfed soil moisture time series. Individual events are correctly captured even if approximately 30 % of the pixel is irrigated.

A quantitative assessment of the detection accuracy achievable with different temporal samplings and irrigated fractions is shown in Fig. 5. The detected irrigation events correspond to actual irrigation, i.e., the precision equals 1, with temporal samplings shorter than 144 h or with irrigated fractions>10 %. However, the number of undetected irrigation events increases, i.e., recall scores worsen, with 24 h revisit time or irrigated fractions smaller than 70 %. Furthermore, the number of undetected events is inversely proportional to the irrigation water amount, i.e., lower irrigation rates cause a higher proportion of undetected irrigation events. For instance, with 48 h (144 h) sampling, only 84 % (42 %) of events are detected when irrigation input is 5 mm/event, compared to 94 % (82 %) when irrigation input is 25 mm/event. A low temporal resolution combined with low irrigation rates leads to a high

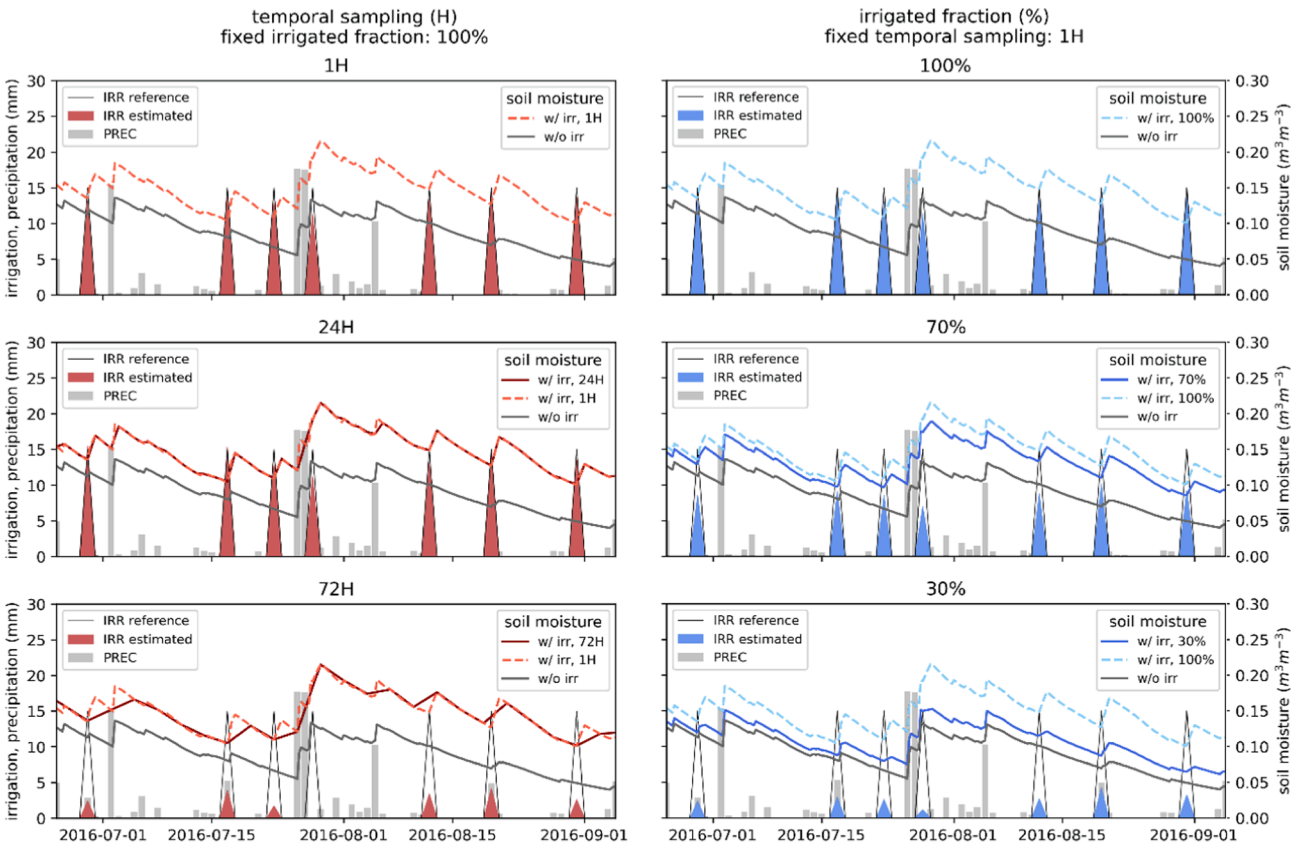

Fig. 4. Soil moisture time series simulated with 15 mm/event irrigation forcing, together with the retrieved irrigation water amounts. Temporally (24 and 72 h, red) and spatially (irrigated fraction of 50 % and 10 %, blue) sub-sampled soil moisture time series are also shown.

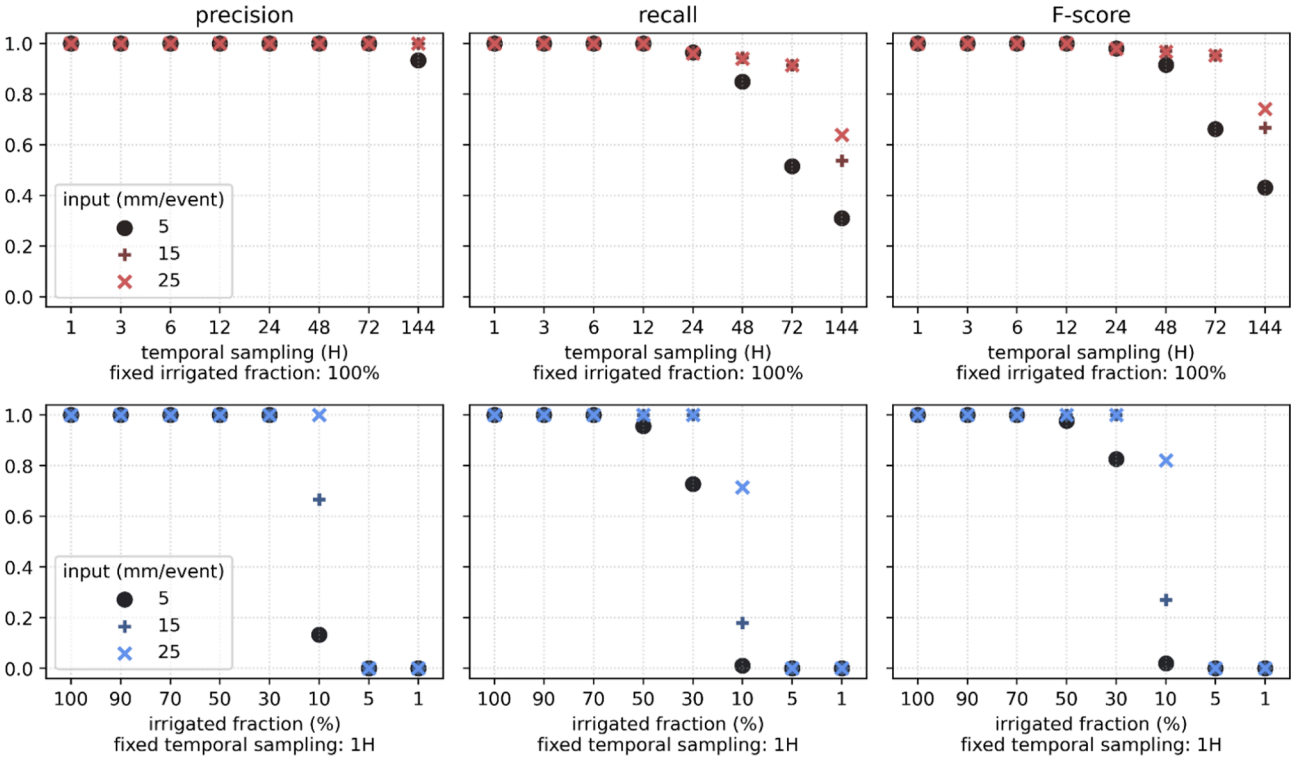

Fig. 5. Detection accuracy expressed as precision, recall, and F-score depending on temporal sampling (top) and irrigated fraction (bottom) of simulated soil moisture. Results are shown for the three irrigation scenarios investigated.

number of missed events. Patterns of the F-score, which provides an overall measure of the detection skill by including false positives and undetected events, indicate good performances for temporal samplings up to 48–72 h. Concerning the irrigated fraction, all events are correctly discriminated (both precision and recall equal 1) when at least half of the pixel is irrigated. When the irrigated fraction lies between 50 % and 10 %, the irrigation rate plays a decisive role in the accuracy scores, especially the recall. For example, with a 10 % irrigated fraction, 72 % of the events are still detected when the irrigation input is 25 mm/event, but recall drops to 19 % when the irrigation rate is 15 mm/event. Analogous results can be observed for the F-score, suggesting that a distinct irrigation-induced signal can be found if at least 30 % of the satellite pixel covers the irrigated field. However, when the irrigated fraction is lower than 10 %, it becomes almost impossible to discriminate individual irrigation events (precision = 0).

Our results corroborate the conclusion reported by various authors that the temporal sampling of most coarse-scale soil moisture products (up to 2–3 days) is suitable for irrigation detection (Brocca et al., 2018; Filippucci et al., 2020; Lawston et al., 2017; Zaussinger et al., 2019). However, coarse resolution products can provide information representative of regional-scale irrigation patterns only if the amount of irrigation water supplied to the soil is sufficient to induce apparent effects on soil moisture, i.e., irrigation is applied extensively within the satellite pixel. On the other hand, field-scale irrigation events cannot be detected with coarse resolution products, as the irrigated fraction of a single field would be significantly lower than 1 %.

Soil moisture products with sub-kilometric spatial resolution, such as those derived from Sentinel-1 (Bauer-Marschallinger et al., 2019; El Hajj et al., 2017), have the potential to provide accurate information about irrigation timing at (quasi) field-scale (Bazzi et al., 2020; Le Page et al., 2020; Zappa et al., 2021). Despite the adequate temporal resolution ensured by the Sentinel-1 mission (1.5–4 days over Europe), low detection accuracy could be obtained because of low irrigation rates. If small amounts of water are supplied to the soil, resulting in a limited impact on the surface water content, satellite observations with high temporal resolution are required to detect irrigation. Furthermore, it is important to highlight that even high spatial resolution products might fail to track irrigation in areas where small fields dominate (e.g., < 5 ha) because of the resulting low irrigated fractions. For instance, with an irrigated field of 5 ha and a satellite pixel with 500 m resolution, the irrigated fraction would be 20 %, hence strongly limiting the detectability of irrigation.

Scatter plots between yearly cumulative reference and estimated irrigation based on the 15 mm/event irrigation scenario are shown in Fig. 6 (similar patterns are found for the 5 and 25 mm/event scenarios). Included are results obtained from the optimal scenario, i.e., soil moisture with hourly resolution and 100 % irrigated fraction, as well as from suboptimal observations, i.e., either temporally sub-sampled or characterized by lower irrigated fractions. We find that with a temporal resolution of 72 h irrigation is largely underestimated, while no considerable differences are observed between hourly and daily sampling. When considering different irrigated fractions, the retrieved irrigation decreases proportionally to the fractional cover of the irrigated area within a pixel. Interestingly, irrigation is underestimated also in the ideal scenario with hourly observations and fully irrigated pixels. This finding stems from the assumption that evapotranspiration and drainage are identical between irrigated and non-irrigated fields (Eq. (6)). However, both fluxes are likely lower over non-irrigated fields, which are generally drier, compared to irrigated fields (Dari, 2021). Hence, estimated irrigation water amounts are expected to be affected by negative biases because differences between these fluxes are not accounted for.

A strong linear relationship (Pearson's $R > 0.85$) is found between estimated and reference irrigation amounts, even with a temporal sampling of 72 h and regardless of the irrigation rate (Fig. 7). With a temporal resolution of 144 h, however, the correlation drops. Extremely low values for both nRMSD and nBIAS are found for temporal samplings from hourly to daily, indicating low errors and low underestimations in the retrieved irrigation, respectively. With revisit times longer than one day, nRMSD and nBIAS deteriorate. In particular, temporal samplings of 72 h (or longer) together with low irrigation rates (5 mm/event) strongly affect the nBIAS, highlighting significant underestimations of the irrigation water amounts. Both nRMSD and nBIAS worsen proportionally to decreasing the irrigated fraction from the optimal scenario, i.e., 100 %, while a good linear correlation between reference and estimated irrigation is also found for irrigated fractions as small as 10 %. This finding suggests that the quantification of irrigation water amounts is strongly limited if only a small portion of a satellite pixel (<10 %) contains the irrigation signal.

Overall, soil moisture observations characterized either by temporal samplings longer than 24 h or irrigated fractions smaller than 50 % lead to sub-optimal irrigation estimates. Most notably, the amount of the retrieved irrigation is consistently lower than the reference irrigation input ($nBIAS < 0$). It should be noted that the estimation of irrigation water amounts is based on the assumption that the various terms of the soil water balance equations are identical at the local and regional scales (see Eqs. (4) and (5)). Despite being a pragmatic assumption simplifying the irrigation retrieval, it can lead to underestimations. In fact, evapotranspiration and drainage are strongly related to the amount of water in the soil. Hence, irrigated fields are likely characterized by higher evapotranspiration and drainage losses compared to the regional dynamics, i.e., rainfed simulations, and these differences are not included in the final irrigation estimates. Furthermore, our findings indicate that the retrieved irrigation water amounts are directly related to the irrigated fraction, i.e., the ratio between the irrigated area within a pixel and the pixel area. Hence, by taking into account spatially explicit maps of irrigated fields (Bazzi et al., 2019; Bousbih et al., 2018; Deines et al., 2019; Gao et al., 2018), systematic irrigation underestimations could be corrected for.

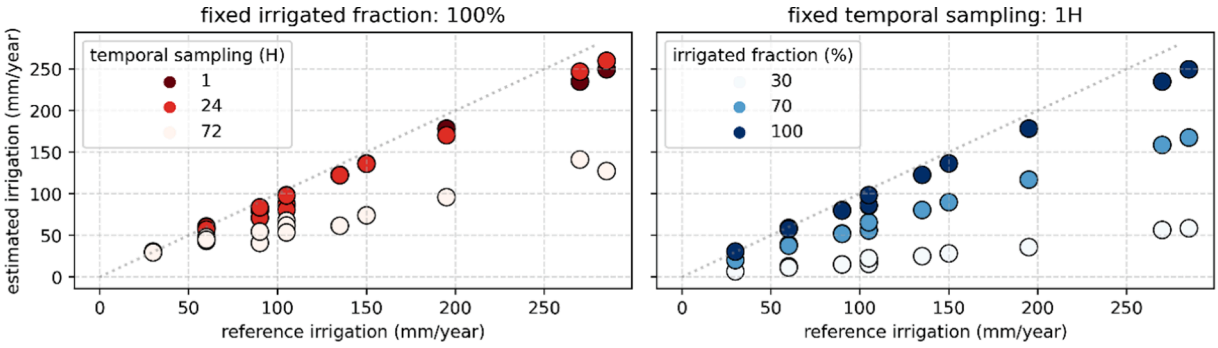

Fig. 6. Comparison between reference and estimated annual irrigation based on different temporal samplings (left) and fractional irrigation coverages (right). Results are shown for the 15 mm/event irrigation scenario.

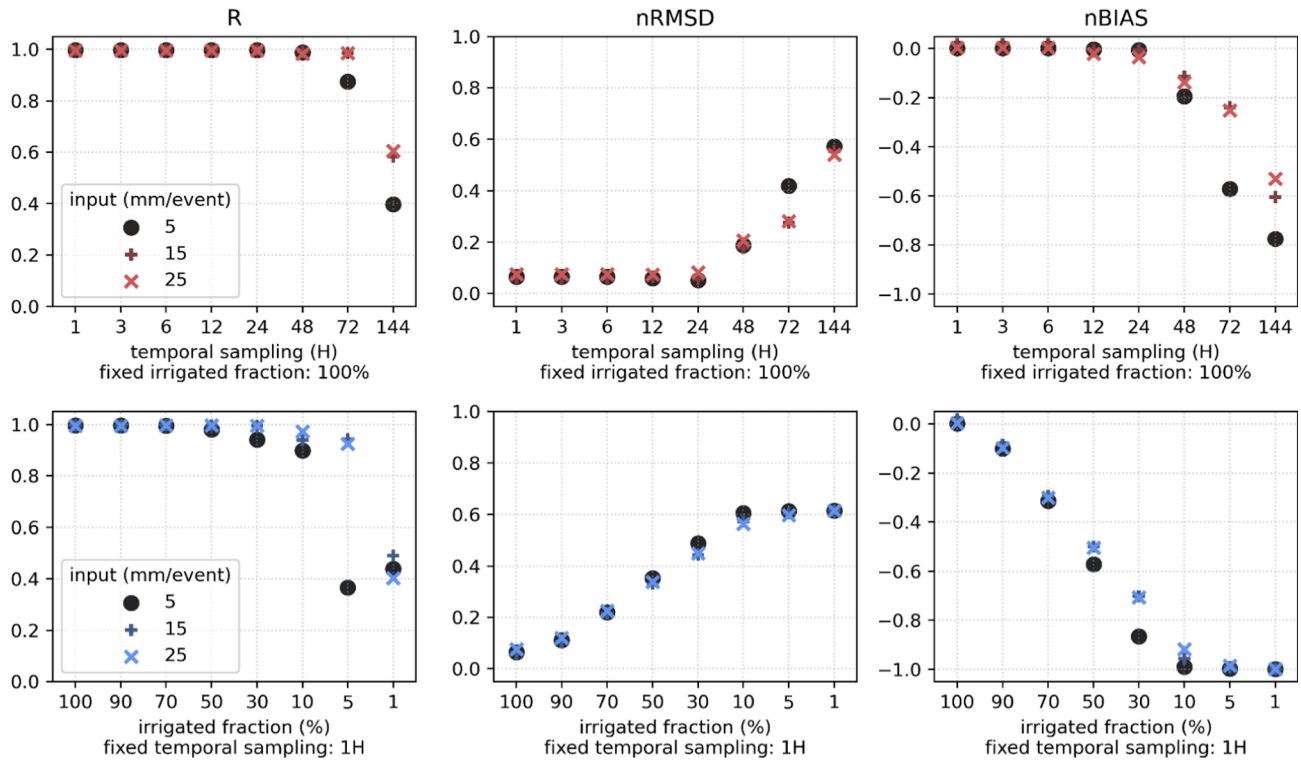

Fig. 7. Quantification accuracy expressed as Pearson's correlation (R), normalized root mean square deviation (nRMSD), and normalized bias (nBIAS) depending on temporal sampling (top) and irrigation fraction (bottom). Results are shown for the three irrigation scenarios investigated.

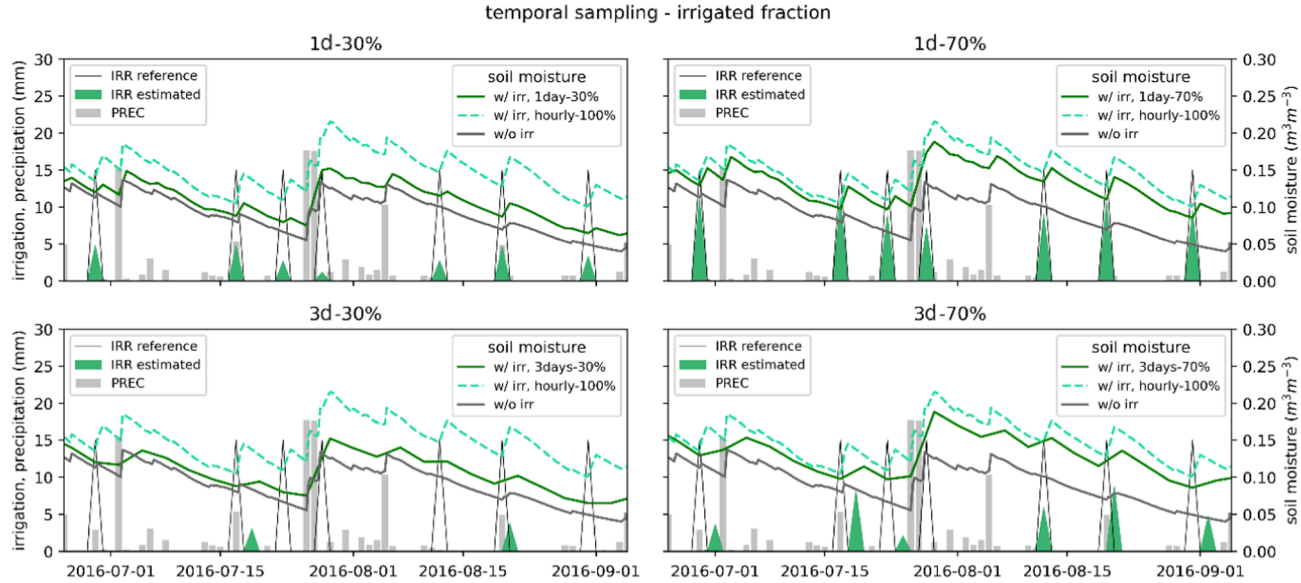

Fig. 8. Soil moisture time series, and corresponding estimated irrigation, based on spatio-temporal resolutions representative of current high-resolution satellite products (1 day – 30 %, 1 day – 70 %, 3 days – 30 %, 3 days – 70 %). Results refer to the 15 mm/event irrigation scenario.

3.2.2. *Combined impact of spatio-temporal resolution and random errors*

Fig. 8 shows soil moisture time series representative of CGLS-SSM-like observational capabilities, i.e., daily (1d) or 3-daily (3d) revisit time and irrigated fraction of 30 % or 70 %. The Sentinel-1 revisit time depends on the acquisition geometry and is location-specific (Bauer-Marschallinger et al., 2019), while the irrigated fraction is subject to the size of the irrigated field(s) covered by a single CGLS-SSM pixel (approximately 80 ha). Hence, an irrigated fraction of 30 % would result from a CGLS-SSM pixel observing an irrigated field of 25 ha, while a 70 % irrigated fraction would translate in, e.g., a CGLS-SSM pixel covering a center pivot field (approximately 55 ha). Note that the soil moisture time series in Fig. 8 do not contain random noise. Only combinations with daily temporal sampling capture the actual soil moisture drying and wetting dynamics, allowing the detection of individual irrigation events. Overall, the concomitant effect of lower spatio-temporal resolution leads to a reduced ability to detect and retrieve irrigation compared to the individual impact of either sub-optimal temporal sampling or irrigated fraction.

Fig. 9 shows the detection skill obtained by the four custom combinations of Fig. 8, without and with the presence of Gaussian noise in the

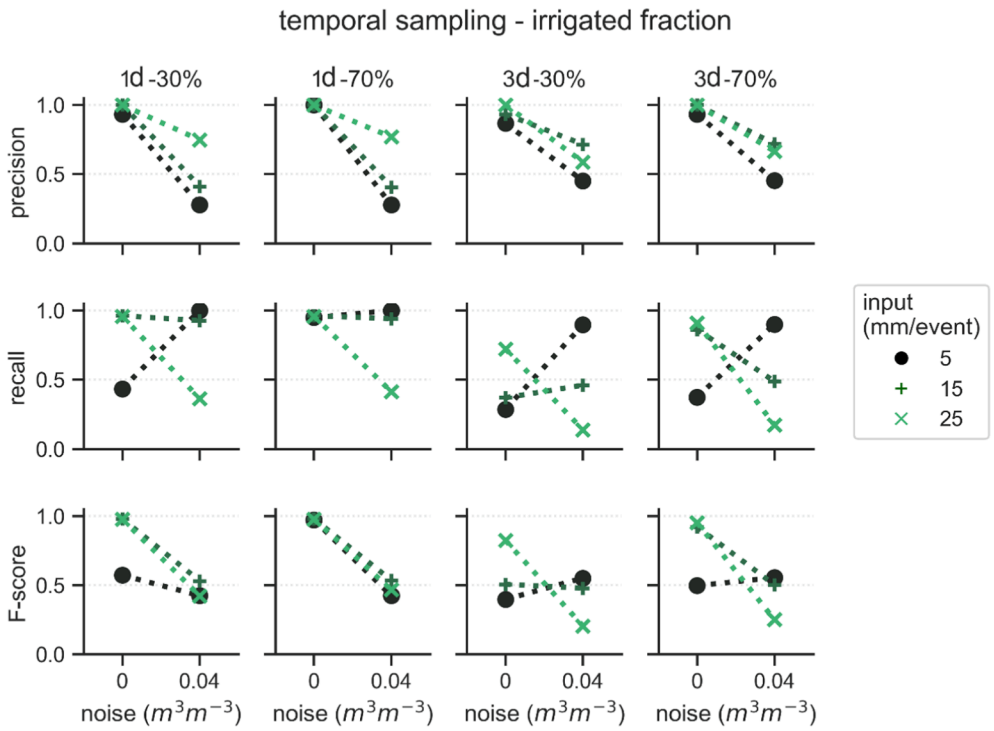

Fig. 9. Detection accuracy obtained with spatio-temporal resolutions representative of current high-resolution satellite products (1 day – 30 %, 1 day – 70 %, 3 days – 30 %, 3 days – 70 %) in the ideal scenario with noise-free observations and after the injection of random errors. The dotted lines are included to highlight the difference between noise-free and noisy observations.

soil moisture time series. With noise-free data, high precision is found regardless of the spatio-temporal combination and irrigation scenario considered. On the other hand, except for the 1d-70 % combination, the recall is lower than 50 %, i.e., more than half of the irrigation events are not detected, when the irrigation is 5 mm/event. With higher irrigation rates, the number of undetected events decreases considerably also for the other combinations. After the addition of random noise, the detection accuracy deteriorates. Interestingly, we find that the recall increases when considering noisy data and low irrigation rates, i.e., 5 mm/event. Such an improvement, however, is an artifact arising from the low detectability of irrigation when small amounts of water are added to the soil. The presence of noise leads to an over-detection of irrigation events,

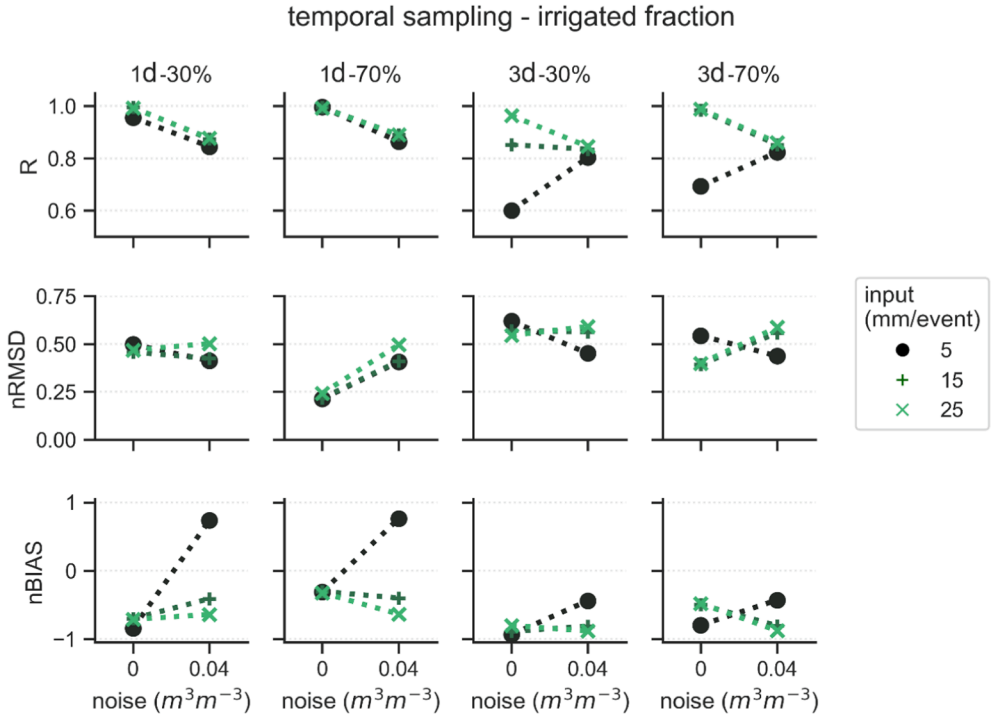

Fig. 10. Quantification accuracy based on spatio-temporal resolutions representative of current high-resolution satellite products (1 day – 30 %, 1 day – 70 %, 3 days – 30 %, 3 days – 70 %) with noise-free soil moisture observations and after the injection of random noise.

resulting on the one hand in a higher recall, i.e., less undetected events, but also lower precision, i.e., more false positive irrigation events. Overall, our results suggest that the presence of noise is particularly detrimental for the detection of irrigation events characterized by medium-to-high irrigation rates, i.e., in those circumstances where the soil moisture differences between irrigated and non-irrigated fields lead to distinct signals.

Fig. 10 summarizes the quantification accuracy achieved by the four custom spatio-temporal combinations. In the ideal scenario with noise-free soil moisture observations, a strong linear relationship (Pearson's $R > 0.8$) is found between reference and estimated irrigation regardless of the combination considered, when the irrigation rate is 15 mm/event or higher. For smaller irrigation volumes, i.e., 5 mm/event, only combinations with daily sampling obtain high R. In terms of nRMSD and nBIAS, the 1d-70 % combination performs considerably better (i.e., nRMSD and nBIAS closer to 0) than all the other combinations. As expected, all the metrics improve with increasing the irrigation rate. The presence of random noise, on the other hand, reduces the differences in quantification accuracy achieved by the four combinations, especially in terms of Pearson's R and nRMSD. A positive nBIAS is found, i.e., irrigation is overestimated, when the irrigation rate is 5 mm/event and the temporal sampling is daily. In these cases, a high number of false positive events, i.e., low precision, were observed (see Fig. 9), leading to largely inflated irrigation estimates. It is noteworthy that nBIAS improves, i.e., becomes closer to 0, also for other scenarios (1d-30 % and 3d-30 %, regardless of irrigation rate). Again, these results are an artifact arising from the stronger contrast between the non-irrigated and the noisy irrigated time series.

Notwithstanding differences in the retrieval approach and test sites, our results agree with the conclusions of Brocca et al. (2018). The authors reported correlation values ranging between 0.78 and 0.95 (0.90 and 0.97), depending on climate (semi-arid versus semi-humid), with an error level of 0.01 $m3/m^{-3}(-|-)$ and considering a yearly irrigation of 300 mm (600 mm). However, the performances degraded after adding random errors to the soil moisture time series.

4. Conclusions

The overall objective of this study was to systematically investigate the impact of soil moisture spatio-temporal resolution on the detection of individual irrigation events and the subsequent quantification of irrigation water amounts. First, satellite soil moisture products were compared to soil moisture simulations obtained using actual irrigation and meteorological data. Then, in a synthetic experiment we thoroughly investigated the effect of soil moisture spatial and temporal resolution, irrigation rate, and presence of noise in the observations, on the accuracy of irrigation estimates. Despite our analysis being limited to a single test site, results obtained here can be generalized to some degree. In fact, we implicitly accounted for the effects of irrigation system, crop type and phenological stage by considering the net irrigation water amounts driving soil moisture dynamics. Also, because of the strong inter-annual climatic variability observed among the period under investigation (2016–2019), our results can be extrapolated to regions characterized by various climates. However, other factors such as individual decisions taken by farmers on, e.g., how often and how long to irrigate, could only be partially simulated as they are highly specific.

The main conclusions that can be drawn based on our results are the following:

- High-resolution satellite soil moisture (the Copernicus Global Land Service Surface Soil Moisture product, CGLS-SSM) agrees better with irrigated soil moisture compared to rainfed simulations, suggesting that CGLS-SSM can potentially be used to monitor irrigation.
- Satisfactory detection skill is found with a temporal resolution of 3 days at most, or if at least one-third of the pixel covers the irrigated field(s), given that soil moisture observations do not contain random errors.
- The irrigation water amounts are systematically underestimated for temporal samplings longer than one day, and decrease proportionally to the irrigated fraction of the pixel, i.e., coarser spatial resolutions lead to larger underestimations.
- The combined effect of lower spatio-temporal resolutions generally causes a decrease in the irrigation retrieval accuracy.
- The detection and quantification accuracies are severely impacted by random noise in the soil moisture time series.
- Performances in the irrigation retrieval are positively related to the amount of water added to the soil, as higher irrigation rates generate a more distinct response in the soil moisture signal.

Overall, our findings indicate that current and upcoming high-resolution satellite soil moisture products only partially meet the spatio-temporal resolution needed for capturing field-scale irrigation signals. The irrigation detection becomes increasingly challenging when the irrigated fraction, i.e., the ratio between field size and satellite pixel resolution, decreases or if low irrigation water volumes are supplied to the field. Furthermore, the retrieval of irrigation information, i.e., timing and water amounts, might be ineffective if (satellite) soil moisture time series contain large errors. Finally, the availability of a more extensive set of in-situ irrigation data, covering a wider range of climatic and environmental conditions and different agricultural practices, is pivotal for the development and validation of irrigation retrieval approaches. Hence, we stress the need for stronger efforts to collect and share in-situ irrigation data.

CRediT authorship contribution statement

Luca Zappa: Conceptualization, Data curation, Formal analysis, Methodology, Writing – original draft, Writing – review & editing. **Stefan Schlaffer:** Methodology, Writing – review & editing. **Luca Brocca:** Data curation, Funding acquisition, Writing – review & editing. **Mariette Vreugdenhil:** Funding acquisition, Writing – review & editing. **Claas Nendel:** Data curation, Writing – review & editing. **Wouter Dorigo:** Funding acquisition, Methodology, Writing – review & editing.

Declaration of Competing Interest

The authors declare that they have no known competing financial interests or personal relationships that could have appeared to influence the work reported in this paper.

Data availability

Data will be made available on request.

Acknowledgments

This research was funded by the European Space Agency through the project IRRIGATION+ (contract number 4000129870/20/I-NB) and the Austrian Research Promotion Agency (FFG) via the DWC-Radar project (project number 873658).

References

Alemohammad, S.H., Kolassa, J., Prigent, C., Aires, F., Gentine, P., 2018. Global downscaling of remotely sensed soil moisture using neural networks. Hydrol. Earth Syst. Sci. 22, 5341–5356. https://doi.org/10.5194/hess-22-5341-2018.

Ambika, A.K., Wardlow, B., Mishra, V., 2016. Remotely sensed high resolution irrigated area mapping in India for 2000 to 2015. Sci. Data 3, 160118. https://doi.org/10.1038/sdata.2016.118.

Amezketa, E., 2006. An integrated methodology for assessing soil salinization, a precondition for land desertification. J. Arid Environ. 67, 594–606. https://doi.org/10.1016/j.jaridenv.2006.03.010.

Anderson, M., 1997. A two-source time-integrated model for estimating surface fluxes using thermal infrared remote sensing. Remote Sens. Environ. 60, 195–216. https://doi.org/10.1016/S0034-4257(96)00215-5.

Ballabio, C., Panagos, P., Monatanarella, L., 2016. Mapping topsoil physical properties at European scale using the LUCAS database. Geoderma 261, 110–123. https://doi.org/10.1016/j.geoderma.2015.07.006.

Bastiaanssen, W.G.M., Menenti, M., Feddes, R.A., Holtslag, A.A.M., 1998. A remote sensing surface energy balance algorithm for land (SEBAL). 1. Formulation. J. Hydrol. 212–213, 198–212. https://doi.org/10.1016/S0022-1694(98)00253-4.

Bauer-Marschallinger, B., Paulik, C., Hochstöger, S., Mistelbauer, T., Modanesi, S., Ciabatta, L., Massari, C., Brocca, L., Wagner, W., 2018. Soil moisture from fusion of scatterometer and SAR: closing the scale gap with temporal filtering. Remote Sens. 10, 1030. https://doi.org/10.3390/rs10071030.

Bauer-Marschallinger, B., Freeman, V., Cao, S., Paulik, C., Schaufler, S., Stachl, T., Modanesi, S., Massari, C., Ciabatta, L., Brocca, L., Wagner, W., 2019. Toward global soil moisture monitoring with Sentinel-1: harnessing assets and overcoming obstacles. IEEE Trans. Geosci. Remote Sens. 57, 520–539. https://doi.org/10.1109/TGRS.2018.2858004.

Bazzi, H., Baghdadi, N., Ienco, D., El Hajj, M., Zribi, M., Belhouchette, H., Escorihuela, M. J., Demarez, V., 2019. Mapping irrigated areas using Sentinel-1 time series in Catalonia, Spain. Remote Sens. 11, 1836. https://doi.org/10.3390/rs11151836.

Bazzi, H., Baghdadi, N., Fayad, I., Zribi, M., Belhouchette, H., Demarez, V., 2020. Near real-time irrigation detection at plot scale using Sentinel-1 Data. Remote Sens. 12, 1456. https://doi.org/10.3390/rs12091456.

Bousbih, S., Zribi, M., Hajj, M.E., Baghdadi, N., Lili-Chabaane, Z., Gao, Q., Fanise, P., 2018. Soil moisture and irrigation mapping in A semi-arid region, based on the synergetic use of Sentinel-1 and Sentinel-2 Data 22.

Brocca, L., Hasenauer, S., Lacava, T., Melone, F., Moramarco, T., Wagner, W., Dorigo, W., Matgen, P., Martínez-Fernández, J., Llorens, P., Latron, J., Martin, C., Bittelli, M., 2011. Soil moisture estimation through ASCAT and AMSR-E sensors: an intercomparison and validation study across Europe. Remote Sens. Environ. 115, 3390–3408. https://doi.org/10.1016/j.rse.2011.08.003.

Brocca, L., Ciabatta, L., Massari, C., Moramarco, T., Hahn, S., Hasenauer, S., Kidd, R., Dorigo, W., Wagner, W., Levizzani, V., 2014. Soil as a natural rain gauge: Estimating global rainfall from satellite soil moisture data: Using the soil as a natural raingauge. J. Geophys. Res. Atmospheres 119, 5128–5141. https://doi.org/10.1002/2014JD021489.

Brocca, L., Ciabatta, L., Moramarco, T., Ponziani, F., Berni, N., Wagner, W., 2016. In: Satellite Soil Moisture Retrieval. Elsevier, pp. 231–247.

Brocca, L., Melone, F., Moramarco, T., 2008. On the estimation of antecedent wetness conditions in rainfall–runoff modelling. Hydrological Processes 22 (5), 629–645. https://doi.org/10.1002/hyp.6629.

Brocca, L., Tarpanelli, A., Filippucci, P., Dorigo, W., Zaussinger, F., Gruber, A., Fernández-Prieto, D., 2018. How much water is used for irrigation? A new approach exploiting coarse resolution satellite soil moisture products. Int. J. Appl. Earth Obs. Geoinformation 73, 752–766. https://doi.org/10.1016/j.jag.2018.08.023.

Brombacher, J., Silva, I.R.d.O., Degen, J., Pelgrum, H., 2022. A novel evapotranspiration based irrigation quantification method using the hydrological similar pixels algorithm. Agric. Water Manag. 267, 107602.

Campbell, B.M., Beare, D.J., Bennett, E.M., Hall-Spencer, J.M., Ingram, J.S.I., Jaramillo, F., Ortiz, R., Ramankutty, N., Sayer, J.A., Shindell, D., 2017. Agriculture production as a major driver of the Earth system exceeding planetary boundaries. Ecol. Soc. 22, art8. https://doi.org/10.5751/ES-09595-220408.

Coleman, R.W., Stavros, N., Hulley, G., Parazoo, N., 2020. Comparison of thermal infrared-derived maps of irrigated and non-irrigated vegetation in urban and non-urban areas of Southern California. Remote Sens. 12, 4102. https://doi.org/10.3390/rs12244102.

Corbari, C., Skokovic Jovanovic, D., Nardella, L., Sobrino, J., Mancini, M., 2020. Evapotranspiration estimates at high spatial and temporal resolutions from an energy-water balance model and satellite data in the Capitanata Irrigation Consortium. Remote Sens. 12, 4083. https://doi.org/10.3390/rs12244083.

Dari, J., Brocca, L., Quintana-Seguí, P., Escorihuela, M.J., Stefan, V., Morbidelli, R., 2020. Exploiting high-resolution remote sensing soil moisture to estimate irrigation water amounts over a mediterranean region. Remote Sens. 12, 2593. https://doi.org/10.3390/rs12162593.

Dari, J., Quintana-Seguí, P., Escorihuela, M.J., Stefan, V., Brocca, L., Morbidelli, R., 2021. Detecting and mapping irrigated areas in a Mediterranean environment by using remote sensing soil moisture and a land surface model. J. Hydrol. 596, 126129.

Deines, J.M., Kendall, A.D., Crowley, M.A., Rapp, J., Cardille, J.A., Hyndman, D.W., 2019. Mapping three decades of annual irrigation across the US high plains aquifer using landsat and google earth engine. Remote Sens. Environ. 233, 111400 https://doi.org/10.1016/j.rse.2019.111400.

Deng, J., Guo, L., Salas, W., Ingraham, P., Charrier-Klobas, J.G., Frolking, S., Li, C., 2018. Changes in irrigation practices likely mitigate nitrous oxide emissions from California cropland. Glob. Biogeochem. Cycles 32, 1514–1527. https://doi.org/10.1029/2018GB005961.

Dong, J., Crow, W.T., 2017. An improved triple collocation analysis algorithm for decomposing autocorrelated and white soil moisture retrieval errors: observation error decomposition. J. Geophys. Res. Atmospheres 122, 13081–13094. https://doi.org/10.1002/2017JD027387.

Dorigo, W., Wagner, W., Albergel, C., Albrecht, F., Balsamo, G., Brocca, L., Chung, D., Ertl, M., Forkel, M., Gruber, A., Haas, E., Hamer, P.D., Hirschi, M., Ikonen, J., de Jeu, R., Kidd, R., Lahoz, W., Liu, Y.Y., Miralles, D., Mistelbauer, T., Nicolai-Shaw, N., Parinussa, R., Pratola, C., Reimer, C., van der Schalie, R., Seneviratne, S.I., Smolander, T., Lecomte, P., 2017. ESA CCI soil moisture for improved Earth system understanding: state-of-the art and future directions. Remote Sens. Environ. 203, 185–215. https://doi.org/10.1016/j.rse.2017.07.001.

Dorigo, W., Dietrich, S., Aires, F., Brocca, L., Carter, S., Cretaux, J.-F., Dunkerley, D., Enomoto, H., Forsberg, R., Güntner, A., Hegglin, M.I., Hollmann, R., Hurst, D.F., Johannessen, J.A., Kummerow, C., Lee, T., Luojus, K., Looser, U., Miralles, D.G., Pellet, V., Recknagel, T., Vargas, C.R., Schneider, U., Schoeneich, P., Schröder, M., Tapper, N., Vuglinsky, V., Wagner, W., Yu, L., Zappa, L., Zemp, M., Aich, V., 2021. Closing the water cycle from observations across scales: where do we stand? Bull. Am. Meteorol. Soc. 102 (10), E1897–E1935.

Droogers, P., Immerzeel, W.W., Lorite, I.J., 2010. Estimating actual irrigation application by remotely sensed evapotranspiration observations. Agric. Water Manag. 97, 1351–1359. https://doi.org/10.1016/j.agwat.2010.03.017.

Eekhout, J.P.C., Hunink, J.E., Terink, W., de Vente, J., 2018. Why increased extreme precipitation under climate change negatively affects water security. Hydrol. Earth Syst. Sci. 22, 5935–5946. https://doi.org/10.5194/hess-22-5935-2018.

El Hajj, M., Baghdadi, N., Zribi, M., Bazzi, H., 2017. Synergic use of Sentinel-1 and Sentinel-2 images for operational soil moisture mapping at high spatial resolution over agricultural areas. Remote Sens. 9, 1292. https://doi.org/10.3390/rs9121292.

Entekhabi, D., Njoku, E.G., O'Neill, P.E., Kellogg, K.H., Crow, W.T., Edelstein, W.N., Entin, J.K., Goodman, S.D., Jackson, T.J., Johnson, J., Kimball, J., Piepmeier, J.R., Koster, R.D., Martin, N., McDonald, K.C., Moghaddam, M., Moran, S., Reichle, R., Shi, J.C., Spencer, M.W., Thurman, S.W., Tsang, L., Van Zyl, J., 2010. The Soil Moisture Active Passive (SMAP) Mission. Proc. IEEE 98, 704–716. https://doi.org/10.1109/JPROC.2010.2043918.

Escorihuela, M.J., Quintana-Seguí, P., 2016. Comparison of remote sensing and simulated soil moisture datasets in Mediterranean landscapes. Remote Sens. Environ. 180, 99–114. https://doi.org/10.1016/j.rse.2016.02.046.

Famiglietti, J.S., 2014. The global groundwater crisis. Nat. Clim. Change 4, 945–948. https://doi.org/10.1038/nclimate2425.

Filippucci, P., Tarpanelli, A., Massari, C., Serafini, A., Strati, V., Alberi, M., Raptis, K.G. C., Mantovani, F., Brocca, L., 2020. Soil moisture as a potential variable for tracking and quantifying irrigation: a case study with proximal gamma-ray spectroscopy data. Adv. Water Resour. 136, 103502 https://doi.org/10.1016/j.advwatres.2019.103502.

Fisher, J.B., Melton, F., Middleton, E., Hain, C., Anderson, M., Allen, R., McCabe, M.F., Hook, S., Baldocchi, D., Townsend, P.A., Kilic, A., Tu, K., Miralles, D.D., Perret, J., Lagouarde, J.-P., Waliser, D., Purdy, A.J., French, A., Schimel, D., Famiglietti, J.S., Stephens, G., Wood, E.F., 2017. The future of evapotranspiration: global requirements for ecosystem functioning, carbon and climate feedbacks, agricultural management, and water resources: the future of evapotranspiration. Water Resour. Res. 53, 2618–2626. https://doi.org/10.1002/2016WR020175.

Foley, J.A., Ramankutty, N., Brauman, K.A., Cassidy, E.S., Gerber, J.S., Johnston, M., Mueller, N.D., O'Connell, C., Ray, D.K., West, P.C., Balzer, C., Bennett, E.M., Carpenter, S.R., Hill, J., Monfreda, C., Polasky, S., Rockström, J., Sheehan, J., Siebert, S., Tilman, D., Zaks, D.P.M., 2011. Solutions for a cultivated planet. Nature 478, 337–342. https://doi.org/10.1038/nature10452.

Gao, Q., Zribi, M., Escorihuela, M.J., Baghdadi, N., Segui, P.Q., 2018. Irrigation Mapping Using Sentinel-1 Time Series at Field Scale 18.

Gruber, A., De Lannoy, G., Albergel, C., Al-Yaari, A., Brocca, L., Calvet, J.-C., Colliander, A., Cosh, M., Crow, W., Dorigo, W., Draper, C., Hirschi, M., Kerr, Y., Konings, A., Lahoz, W., McColl, K., Montzka, C., Muñoz-Sabater, J., Peng, J., Reichle, R., Richaume, P., Rüdiger, C., Scanlon, T., van der Schalie, R., Wigneron, J.-P., Wagner, W., 2020. Validation practices for satellite soil moisture retrievals: What are (the) errors? Remote Sens. Environ. 244, 111806 https://doi.org/10.1016/j.rse.2020.111806.

Hain, C.R., Crow, W.T., Anderson, M.C., Yilmaz, M.T., 2015. Diagnosing neglected soil moisture source-sink processes via a thermal infrared-based two-source energy balance model. J. Hydrometeorol. 16, 1070–1086. https://doi.org/10.1175/JHM-D-14-0017.1.

Jalilvand, E., Tajrishy, M., Hashemi, S.A.G.Z., Brocca, L., 2019. Quantification of irrigation water using remote sensing of soil moisture in a semi-arid region. Remote Sens. Environ. 231 https://doi.org/10.1016/j.rse.2019.111226.

Kumar, S.V., Peters-Lidard, C.D., Santanello, J.A., Reichle, R.H., Draper, C.S., Koster, R. D., Nearing, G., Jasinski, M.F., 2015. Evaluating the utility of satellite soil moisture retrievals over irrigated areas and the ability of land data assimilation methods to correct for unmodeled processes. Hydrol. Earth Syst. Sci. 19, 4463–4478. https://doi.org/10.5194/hess-19-4463-2015.

Kummu, M., Guillaume, J.H.A., de Moel, H., Eisner, S., Flörke, M., Porkka, M., Siebert, S., Veldkamp, T.I.E., Ward, P.J., 2016. The world's road to water scarcity: shortage and stress in the 20th century and pathways towards sustainability. Sci. Rep. 6, 38495. https://doi.org/10.1038/srep38495.

Lawston, P.M., Santanello, J.A., Kumar, S.V., 2017. Irrigation signals detected from SMAP soil moisture retrievals: irrigation signals detected From SMAP. Geophys. Res. Lett. 44, 11860–11867. https://doi.org/10.1002/2017GL075733.

Le Page, M., Jarlan, L., El Hajj, M.M., Zribi, M., Baghdadi, N., Boone, A., 2020. Potential for the detection of irrigation events on maize plots using Sentinel-1 soil moisture products. Remote Sens. 12, 1621. https://doi.org/10.3390/rs12101621.

Lopez, O., Johansen, K., Aragon, B., Li, T., Houborg, R., Malbeteau, Y., AlMashharawi, S., Altaf, M.U., Fallatah, E.M., Dasari, H.P., Hoteit, I., McCabe, M.F., 2020. Mapping groundwater abstractions from irrigated agriculture: big data, inverse modeling and a satellite-model fusion approach (preprint). Water Resources Manage./Remote Sens. GIS. https://doi.org/10.5194/hess-2020-50.

Malbéteau, Y., Merlin, O., Balsamo, G., Er-Raki, S., Khabba, S., Walker, J.P., Jarlan, L., 2018. Toward a surface soil moisture product at high spatiotemporal resolution: temporally interpolated, spatially disaggregated SMOS data. J. Hydrometeorol. 19, 183–200. https://doi.org/10.1175/JHM-D-16-0280.1.

Massari, C., Modanesi, S., Dari, J., Gruber, A., De Lannoy, G.J.M., Girotto, M., Quintana-Seguí, P., Le Page, M., Jarlan, L., Zribi, M., Ouaadi, N., Vreugdenhil, M., Zappa, L., Dorigo, W., Wagner, W., Brombacher, J., Pelgrum, H., Jaquot, P., Freeman, V., Volden, E., Fernandez Prieto, D., Tarpanelli, A., Barbetta, S., Brocca, L., 2021. A review of irrigation information retrievals from space and their utility for users. Remote Sens. 13, 4112. https://doi.org/10.3390/rs13204112.

McCabe, M.F., Ershadi, A., Jimenez, C., Miralles, D.G., Michel, D., Wood, E.F., 2016. The GEWEX LandFlux project: evaluation of model evaporation using tower-based and globally gridded forcing data. Geosci. Model Dev. 9, 283–305. https://doi.org/10.5194/gmd-9-283-2016.

McCabe, M.F., Miralles, D.G., Holmes, T.R.H., Fisher, J.B., 2019. Advances in the remote sensing of terrestrial evaporation. Remote Sens. 11, 1138. https://doi.org/10.3390/rs11091138.

Meier, J., Zabel, F., Mauser, W., 2018. A global approach to estimate irrigated areas – a comparison between different data and statistics. Hydrol. Earth Syst. Sci. 22, 1119–1133. https://doi.org/10.5194/hess-22-1119-2018.

Melone, F., Corradini, C., Morbidelli, R., Saltalippi, C., Flammini, A., 2008. Comparison of theoretical and experimental soil moisture profiles under complex rainfall patterns. J. Hydrol. Eng. 13, 1170–1176. https://doi.org/10.1061/(ASCE)1084-0699(2008)13:12(1170).

Miralles, D.G., Jiménez, C., Jung, M., Michel, D., Ershadi, A., McCabe, M.F., Hirschi, M., Martens, B., Dolman, A.J., Fisher, J.B., Mu, Q., Seneviratne, S.I., Wood, E.F., Fernández-Prieto, D., 2016. The WACMOS-ET project – Part 2: Evaluation of global terrestrial evaporation data sets. Hydrol. Earth Syst. Sci. 20, 823–842. https://doi.org/10.5194/hess-20-823-2016.

Modanesi, S., Massari, C., Bechtold, M., Lievens, H., Tarpanelli, A., Brocca, L., Zappa, L., De Lannoy, G.J.M., 2022. Challenges and benefits of quantifying irrigation through the assimilation of Sentinel-1 backscatter observations into Noah-MP (preprint). Water Resources Manage./Modelling Approaches. https://doi.org/10.5194/hess-2022-61.

Morbidelli, R., Corradini, C., Saltalippi, C., Flammini, A., Rossi, E., 2011. Infiltration-soil moisture redistribution under natural conditions: experimental evidence as a guideline for realizing simulation models. Hydrol. Earth Syst. Sci. 15, 2937–2945. https://doi.org/10.5194/hess-15-2937-2011.

Ozdogan, M., Gutman, G., 2008. A new methodology to map irrigated areas using multi-temporal MODIS and ancillary data: an application example in the continental US. Remote Sens. Environ. 112, 3520–3537. https://doi.org/10.1016/j.rse.2008.04.010.

Peña-Arancibia, J.L., Mainuddin, M., Kirby, J.M., Chiew, F.H.S., McVicar, T.R., Vaze, J., 2016. Assessing irrigated agriculture's surface water and groundwater consumption by combining satellite remote sensing and hydrologic modelling. Sci. Total Environ. 542, 372–382. https://doi.org/10.1016/j.scitotenv.2015.10.086.

Peng, J., Loew, A., Merlin, O., Verhoest, N.E.C., 2017. A review of spatial downscaling of satellite remotely sensed soil moisture: downscale satellite-based soil moisture. Rev. Geophys. 55, 341–366. https://doi.org/10.1002/2016RG000543.

Puy, A., Sheikholeslami, R., Gupta, H.V., Hall, J.W., Lankford, B., Lo Piano, S., Meier, J., Pappenberger, F., Porporato, A., Vico, G., Saltelli, A., 2022. The delusive accuracy of global irrigation water withdrawal estimates. Nat. Commun. 13, 3183. https://doi.org/10.1038/s41467-022-30731-8.

Qiu, J., Gao, Q., Wang, S., Su, Z., 2016. Comparison of temporal trends from multiple soil moisture data sets and precipitation: the implication of irrigation on regional soil moisture trend. Int. J. Appl. Earth Obs. Geoinformation 48, 17–27. https://doi.org/10.1016/j.jag.2015.11.012.

Reyes-Cabrera, J., Zotarelli, L., Dukes, M.D., Rowland, D.L., Sargent, S.A., 2016. Soil moisture distribution under drip irrigation and seepage for potato production. Agric. Water Manag. 169, 183–192. https://doi.org/10.1016/j.agwat.2016.03.001.

Rockström, J., Falkenmark, M., Lannerstad, M., Karlberg, L., 2012. The planetary water drama: Dual task of feeding humanity and curbing climate change: frontier. Geophys. Res. Lett. 39 https://doi.org/10.1029/2012GL051688.

Romaguera, M., Hoekstra, A.Y., Su, Z., Krol, M.S., Salama, Mhd.S., 2010. Potential of Using Remote Sensing Techniques for Global Assessment of Water Footprint of Crops. Remote Sens. 2, 1177–1196. https://doi.org/10.3390/rs2041177.

Rubel, F., Brugger, K., Haslinger, K., Auer, I., 2017. The climate of the European Alps: shift of very high resolution Köppen-Geiger climate zones 1800–2100. Meteorol. Z. 26 (2), 115–125.

Sabaghy, S., Walker, J.P., Renzullo, L.J., Jackson, T.J., 2018. Spatially enhanced passive microwave derived soil moisture: Capabilities and opportunities. Remote Sens. Environ. 209, 551–580. https://doi.org/10.1016/j.rse.2018.02.065.

Siebert, S., Döll, P., 2010. Quantifying blue and green virtual water contents in global crop production as well as potential production losses without irrigation. J. Hydrol. 384, 198–217. https://doi.org/10.1016/j.jhydrol.2009.07.031.

Thenkabail, P.S., Biradar, C.M., Noojipady, P., Dheeravath, V., Li, Y., Velpuri, M., Gumma, M., Gangalakunta, O.R.P., Turral, H., Cai, X., Vithanage, J., Schull, M.A., Dutta, R., 2009. Global irrigated area map (GIAM), derived from remote sensing, for the end of the last millennium. Int. J. Remote Sens. 30, 3679–3733. https://doi.org/10.1080/01431160802698919.

van Dijk, A.I.J.M., Schellekens, J., Yebra, M., Beck, H.E., Renzullo, L.J., Weerts, A., Donchyts, G., 2018. Global 5 km resolution estimates of secondary evaporation including irrigation through satellite data assimilation. Hydrol. Earth Syst. Sci. 22, 4959–4980. https://doi.org/10.5194/hess-22-4959-2018.

van Eekelen, M.W., Bastiaanssen, W.G.M., Jarmain, C., Jackson, B., Ferreira, F., van der Zaag, P., Saraiva Okello, A., Bosch, J., Dye, P., Bastidas-Obando, E., Dost, R.J.J., Luxemburg, W.M.J., 2015. A novel approach to estimate direct and indirect water withdrawals from satellite measurements: a case study from the Incomati basin. Agric. Ecosyst. Environ. 200, 126–142. https://doi.org/10.1016/j.agee.2014.10.023.

Vörösmarty, C.J., Green, P., Salisbury, J., Lammers, R.B., 2000. Global water resources: vulnerability from climate change and population growth. Science 289 (5477), 284–288.

Wada, Y., van Beek, L.P.H., Bierkens, M.F.P., 2012. Nonsustainable groundwater sustaining irrigation: a global assessment: nonsustainable groundwater sustaining irrigation. Water Resour. Res. 48 https://doi.org/10.1029/2011WR010562.

Wriedt, G., van der Velde, M., Aloe, A., Bouraoui, F., 2009. A European irrigation map for spatially distributed agricultural modelling. Agric. Water Manag. 96, 771–789. https://doi.org/10.1016/j.agwat.2008.10.012.

Zappa, L., Forkel, M., Xaver, A., Dorigo, W., 2019. Deriving field scale soil moisture from satellite observations and ground measurements in a hilly agricultural region. Remote Sens. 11, 2596. https://doi.org/10.3390/rs11222596.

Zappa, L., Schlaffer, S., Bauer-Marschallinger, B., Nendel, C., Zimmerman, B., Dorigo, W., 2021. Detection and quantification of irrigation water amounts at 500 m using Sentinel-1 surface soil moisture. Remote Sens. 13, 1727. https://doi.org/10.3390/rs13091727.

Zaussinger, F., Dorigo, W., Gruber, A., Tarpanelli, A., Filippucci, P., Brocca, L., 2019. Estimating irrigation water use over the contiguous United States by combining satellite and reanalysis soil moisture data. Hydrol. Earth Syst. Sci. 23, 897–923. https://doi.org/10.5194/hess-23-897-2019.

Zhang, X., Qiu, J., Leng, G., Yang, Y., Gao, Q., Fan, Y., Luo, J., 2018. The potential utility of satellite soil moisture retrievals for detecting irrigation patterns in China. Water 10, 1505. https://doi.org/10.3390/w10111505.

Zohaib, M., Choi, M., 2020. Satellite-based global-scale irrigation water use and its contemporary trends. Sci. Total Environ. 714, 136719 https://doi.org/10.1016/j.scitotenv.2020.136719.

Zohaib, M., Kim, H., Choi, M., 2019. Detecting global irrigated areas by using satellite and reanalysis products. Sci. Total Environ. 677, 679–691. https://doi.org/10.1016/j.scitotenv.2019.04.365.

Zwieback, S., Dorigo, W., Wagner, W., 2013. Estimation of the temporal autocorrelation structure by the collocation technique with an emphasis on soil moisture studies. Hydrol. Sci. J. 58, 1729–1747. https://doi.org/10.1080/02626667.2013.839876.